Smart Geotechnics for Smart Societies – Zhussupbekov, Sarsembayeva & Kaliakin (Eds)

Undrained instability and fluidization of soft subgrade soils under cyclic rail loading

B. Indraratna, T.T. Nguyen, J. Arivalagan, M. Singh, C. Rujikiatkamjorn & T. Doan
Transport Research Centre, Faculty of Engineering & Information Technology, University of Technology Sydney, Australia

ABSTRACT: The rapidly increasing demand for rail infrastructure to transport passengers and freight has inevitably led to a need for more robust and sustainable track foundations. However, heavy haul rail tracks often run across unfavourable soil conditions (e.g., saturated soft estuarine soils), resulting in frequent track failures accompanied with high maintenance cost. Recent site investigations along the South Coast rail line (NSW, Australia) showed considerable track degradation induced by subgrade mud pumping, requiring urgent attention and studies. This paper thus presents extensive laboratory and numerical investigations on the mechanism and possible solutions for mud pumping. While the effects of mud pumping on track performance are investigated through large-scale permeability and shear tests using the collected fouled ballast, the subgrade soil is subjected to cyclic triaxial and large-scale cyclic testing to understand the soil fluidization and fine particle migration. Transducers are installed at different layers to observe the depth-dependent response of soil foundation under various conditions. The results show that when specimens are subjected to unfavourable cyclic stresses, the fine particles migrate from the lower toward the upper soil layers along with the redistribution of pore water. When the water content of the upper soil layer reaches the liquid limit, the top of the specimen transforms into a slurry. Micro-analysis based on CFD-DEM coupling indicates a serious degradation in soil fabric and strength, thus the formation of mud under rising excess pore water pressure (EPWP). The study indicates that adding reasonable mass of cohesive fines can enhance the resistance of subgrade soils to fluidization, while geotextiles and geocomposites can also be used to mitigate mud pumping. Prefabricated vertical drains (PVDs) can continually reduce the buildup of EPWPs over the time due to the substantial reduction in drainage path, suggesting the efficiency of using the combined PVD-geocomposite system to mitigate mud pumping.

1 INTRODUCTION

1.1 *Subgrade failure under heavy freight trains*

In recent decades, the demand for faster and heavier freight transportation has pressurized geotechnical engineers worldwide to establish more robust and resilient rail track foundations. Alongside countries such as China, the USA, the UK, Canada and other European regions, Australian railways is one of the largest networks with rapid development in transport capacity. For example, the average train length is between 2-4 km, while the axle load is commonly 30 to 40 tonnes on mining and agricultural demands (Indraratna et al. 2014). However, this also results in devastating effects on the stability and longevity of track foundations, causing a greater degree of track deformation and foundation failures. In coastal regions where soft and saturated soils are prevalent, the repeated passage of heavy haul trains with increasing axle loads has been shown to exacerbate the accumulated excess pore water pressure (EPWP) and plastic deformation. When EPWP develops non-uniformly along the depth (localized response), it can stimulate the migration of pore water associated with fines, thus the formation of slurry track, i.e., mud pumping. The

DOI: 10.1201/9781003299127-2

infiltrated fines result in fouling of the ballast, reducing the interlocking between ballast particles (i.e., reduced shear strength) and impeding the drainage capacity (i.e., clogging) of the track foundation (Nguyen et al. 2019). Recent field inspections (Nguyen and Indraratna 2022c) have revealed a significant number of slurry sites along the South Coast (SC) rail line, NSW (Figure 1), many of which often repeat over year despite considerable maintenance cost. In low-lying regions, subgrade soil can be pushed upward (i.e., heave failure) under rising EPWP, seriously deteriorating structure and load bearing capacity of the track foundation. Hence, this phenomenon urgently demands a comprehensive investigation and feasible solutions.

Conventional studies (Selig and Waters 1994) indicated 3 different failure types of subgrade under rail tracks, i.e., (i) massive shear failure, (ii) progressive shear failure and (iii) attrition. However, these do not include the mechanism that transforms subgrade into fluid-like state. Furthermore, the internal migration of fines and moisture along the subgrade depth under repeated loads was not usually attended properly in past studies. Considerable effort has therefore gone to characterizing this phenomenon in the recent years (Duong et al. 2013; Chawla and Shahu 2016; Indraratna et al. 2020a). Past investigations (Hyodo et al. 1994; Indraratna et al. 2020a) indicated that the undrained shear failure can be characterized by the progressive advancement of excess pore water pressure and axial strain until the stress envelope reaches a failure line. On the other hand, when subjected to fluidization, soil becomes softened and fails under internal migration of pore water and fines, followed by the degradation in the stiffness and fabric of the specimens (Indraratna et al. 2020b; Nguyen et al. 2022). Subgrade instability is normally governed by complex combinations of internal and external factors. The internal factors can arise from soil characteristics such as particle size distribution, plasticity index (PI), void ratio and initial fabric (Vucetic and Dobry 1991; Polito and II 2001; Silva et al. 2022), whereas the external influences include the loading state and drainage condition (Sakai et al. 2003; Nguyen et al. 2019). Indraratna et al. (2020a) show that adding cohesive fines as well as increasing compaction degree can enhance soil resistance to fluidization. Despite abundant studies have been conducted to investigate the response of subgrade soils under repeated loads, the mechanism and causative factors that trigger the internal migration of soil particles and moisture still needs further explanation.

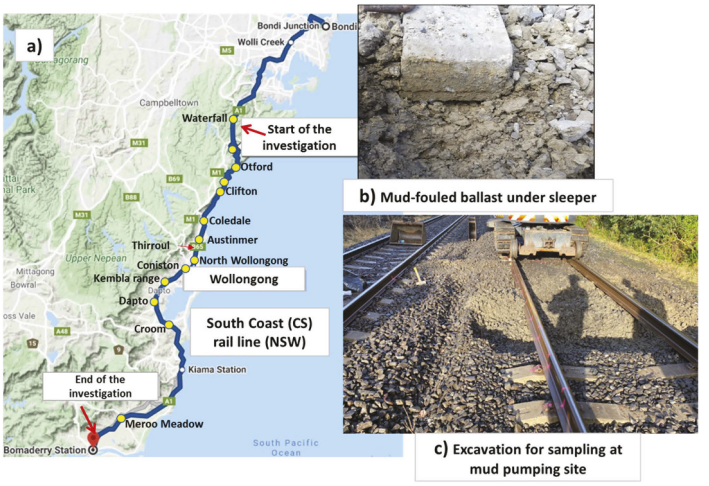

Figure 1. Field inspections of mud pumping sites including (a) locations along the South Coast (SC) line; (b) visual inspection of cohesive fines in ballast layer; and c) excavation for sampling.

1.2 *Use of geosynthetics to stabilize railway foundation*

Although a variety of solutions have been introduced, the most reliable and cost-effective solution for mud pumping and subgrade instability is still a critical question. The common practical method used to remediate a mud pumping track is replacement of the fouled ballast, however, this cannot always prevent the risk caused by subgrade mud pumping (Hudson et al.

2016). Increasing the thickness of ballast or renewing the subgrade (slurry) are expensive, but they are currently used in practice due to the simplicity and long-life effectiveness (Transport for NSW 2016). Additives such as lime and fly ash can also be used to increase the stability and cyclic resistance of substructures, they are time consuming and complex in construction while causing significant environmental impacts (Nguyen et al. 2019).

Geosynthetics are also commonly used to mitigate the migration of soil under railway and highways. Geotextiles have been used as a separation and filter layer under rail tracks for several decades, however, their effectiveness in preventing mud pumping is still now under debate (Raymond 1986; Sharpe et al. 2014; Hudson et al. 2016). Prefabricated vertical drains (PVDs) have been proved as a cost-effective method to shorten drainage path, thus accelerating the dissipation of EPWP as well as mitigating mud pumping (Indraratna et al. 2009; Singh et al. 2020). Short PVDs, i.e., installed in shallow depths within 6-8 m can prevent the accumulation of EPWP induced by the passage of heavy trains, meaning the less susceptibility of subgrade soil to internal instability. Furthermore, horizontal (i.e., transverse) drains can also be installed to facilitate drainage, thereby dissipating EPWP induced by train loads (Ito 1984).

Figure 2 shows the application of geocomposite material to prevent the migration of soil particles and associated mud pumping at Chullora, New South Wales (NSW). Although various geotextiles and geocomposites have been tested in the field and undergone large-scale laboratory testing, their effectiveness to prevent particle migration and fluidization varies widely. Some studies reported that geosynthetics have a limited efficiency and their performance could diminish quite significantly over the years (Selig and Waters 1994; Sharpe et al. 2014). Recent studies show that the installation of effective geosynthetics could prevent particle migration and potential track failures under dynamic loading (Lenart et al. 2018; Kermani et al. 2020). However, the use of geotextile allowed for in-plane drainage and dissipated the rapid development of EPWP. The pore arrangement in geotextiles should be large enough to provide adequate seepage (drainage capacity) and yet small enough to prevent particle migration (filtration) (Giroud 1996). Preventing particles from infiltrating into the overlying layers can increase the permeability of the drainage layer and provide continuous performance under loads.

Figure 2. Geocomposite installation to mitigate the fluidization potential of soft soil at Chullora, New South Wales (an ongoing pilot study supported by Sydney Trains).

This paper aims to review recent state-of-the-art studies around subgrade soil fluidization and the use of geosynthetics and geocomposites to prevent this failure under heavy haul rail tracks. Laboratory investigations from elemental to large scale model tests using real soil samples collected from mud pumping sites in NSW, Australia were extensively carried out at Transport Research Centre (TRC), UTS in recent years. Numerical model was also implemented to provide an insight into the micro-mechanism of soil fluidization under rising internal hydraulic gradient.

2 RESEARCH METHODOLOGY

2.1 *Cyclic triaxial tests*

It is critical to study the cyclic behavior of the subgrade soils prone to undrained instability and fluidization at a fundamental approach such as cyclic triaxial test. Disturbed soil samples were collected from several locations near Wollongong City. Basic geotechnical tests characterized the soils as low plastic clay, CL having a liquid limit less than 30 and a plasticity index of nearly 11. It is anticipated that low-medium plastic soils (PI < 26) are inherently vulnerable to mud pump due to the low cohesion between the soil particles (Duong et al. 2013; Chawla and Shahu 2016; Nguyen et al. 2019; Indraratna et al. 2020b). To achieve uniformity in sample preparation, the soil samples were compacted to a desired density ρ_d = 1600, 1680 and 1790 kg/m^3) using non-linear under-compaction criterion. The ratio of the initial specimen density to the maximum dry density of the soil is defined as Relative compaction (RC). The readers are referred to the following publication (Indraratna et al. 2020b) for further details on sample preparation.

To investigate the cyclic behavior of the reconstituted specimens, a series of stress-controlled undrained cyclic triaxial tests were performed using the GDS ELDYN dynamic triaxial testing equipment. The ELDYN system employs a pneumatic controller to apply the desired confining pressure. The pore pressure response was measured by employing a pore pressure transducer at the bottom of the specimen. Further, site investigations have revealed that mud pumping is a shallow phenomenon, therefore, the specimens were subjected to an effective confining pressure of σ'_{3c} = 15 kPa to simulate the shallow subgrade region. All specimens were back-saturated at a pressure of 400 kPa and then subjected to anisotropic consolidation (k_0 = 0.6).

The effect of varying axle loads was simulated by varying the cyclic stress ratio (CSR) from 0.2 to 1.0. The cyclic stress ratio (CSR) is defined as the ratio of the applied dynamic stress σ_d to twice of the effective confining pressure σ'_{3c}. The loading resulting from the passage of the trains was simulated through a sinusoidal waveform. The specimens were subjected to varying loading frequency (1.0 to 5.0 Hz) and the tests were concluded when the specimens experienced 5% cyclic axial strain or 50000 loading cycles. A generic representation for the fluidized specimen is highlighted in Figure 3 and the formation of a slurry at the top of the specimen at higher CSRs can be visually observed.

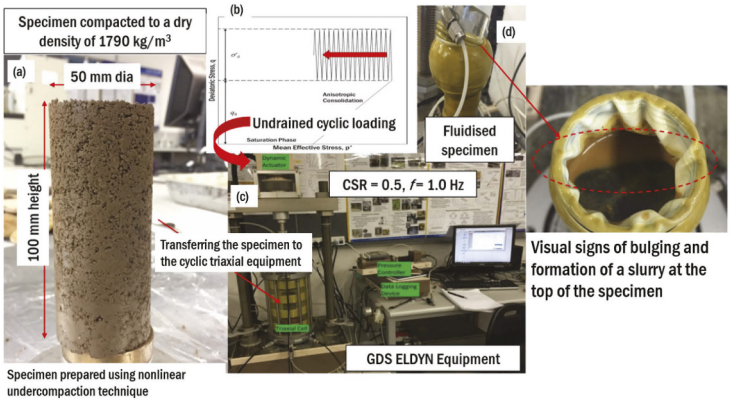

Figure 3. (a) Reconstituted specimen (b) Schematic for undrained loading (c) Cyclic triaxial rig (d) Typical fluidized specimen.

2.2 *Large-scale dynamic tests*

In order to capture the localized behaviour of subgrade soil as well as examining the efficiency of using geocomposite to stabilize subgrade soil under heavy cyclic loading, a series of large-scale dynamic tests were carried out at TRC.

2.2.1 *Testing materials*

Soil samples that had experienced mud pumping were collected from Wollongong, South Coast Rail line (NSW, Australia) for this study. The liquid limit (LL) and plastic limit (PL) of the soil were 42% and 26%, respectively and this soil could be classified as inorganic clay with medium plasticity. The maximum dry density (MDD) and optimum moisture content (OMC) were 1,682 kg/m^3 and 18.5%, respectively. The average water content after saturation was around 32% and the specific gravity was 2.59. A perspex hydraulic cell with a diameter (internal) of 140 mm and a height of 300 mm was used for the permeability tests. D_{cell}/D_{100} is greater than 42 and could avoid the effects of boundary wall friction (i.e. the ratio between the largest particle and the internal diameter of the cell is less than 1⁄6 (ASTM D3999-91 2003)). The compacted soil had a permeability of 8.9x10^{-7} m/s, as determined using the falling head method. Geotextiles and geocomposites with pore opening sizes of 10 to 80 μm, were used for the laboratory experiments. Geocomposite (T1) had a filter which sandwiched between two nonwoven geotextile layers with aperture opening sizes (O_{95}) of <10 μm. Prefabricated vertical drains (PVDs) had an assembled drain width of 100 mm, a thickness of 3.4 mm, and a drain filter pore size of 75 μm. All the properties of the geotextiles and PVD are listed in Table 1.

Table 1. Specification of geosynthetics used in the current.

Geotextile/geocomposite	T1*	T2	PVD	P
Tensile strength (EN ISO 10319 2008)	95 kN/m	22 kN/m	Drain Core and Filter material	PP and PET
CBR resistance (EN ISO 12236 2006)	18 kN	4.3 kN	Assembled drain width (ASTM D3774-96 1996)	100 mm
Pore size – Mean AOS (ASTM F316-03 2011)	<10 μm	60 μm	Assembled drain thickness (ASTM D5199-01 2001)	3.4 mm
Permeability (EN ISO 11058 2019)	0.35 l/m^{2}s	30 l/m^{2}s	Grab strength (ASTM D638-03 2003)	2.5 kN
Thickness (EN ISO 9863-1 2005)	9 mm	2 mm	Drain flow discharge (ASTM D4716-00 2000) at 200 kPa	2800 m^3/yr
Cone drop (EN ISO 13433 2006)	0 mm	22 mm	Drain filter pore size (ASTM D4751-99 1999)	75 μm

* - geocomposite

2.2.2 *Testing apparatus*

The Dynamic Filtration Apparatus (DFA) was designed at the University of Technology Sydney (UTS), Australia, to monitor the local EPWPs, soil porosity, development of excess pore pressure gradients (EPPGs) between different soil layers, and axial deformation under cyclic loading conditions (Figure 4). Four MPs with 1 kPa accuracy were placed on the center-line of the subgrade specimen at depths of 20, 40, 80, and 120 mm from the ballast/subgrade interface. Six pressure transducers (accuracy 0.5 kPa) were placed at the edge of cylinder at depths of 25, 55, 85, 115, 145, and 175 mm away from the ballast/subgrade interface. The local EPPGs that developed inside the specimen was calculated by measuring the differential hydraulic pressure at each layer. Amplitude Domain Reflectometry (ADR) probes were also installed along the subgrade depths and the variations in porosity could be monitored using the dynamic filtration apparatus (Arivalagan et al. 2021).

2.2.3 *Test procedures*

The collected soil from a mud pumping site was sieved through 2.36 mm. The target bulk density (1600 kg/m^3) and moisture content (17%) were achieved by compacting the dry soil and water to the desired volume. The 'nonlinear under-compaction' criterion was adopted to obtain a uniform density for the test specimen. PVDs with a modified size were used in the experiments based on the time factor and the average degree of consolidation for two soil cylinders, as proposed by (Ni 2012; Abeywickrama et al. 2021). Saturation was done with

filtered and de-aired water and monitored continuously by three ADR probes installed at different depths. A uniform vertical pressure of 30 kPa was applied to consolidate the soil specimen. The pore pressure that developed during consolidation process was monitored, and the settlement due to the applied loading was recorded continuously for two days. The geotextile was saturated before being placed onto the subgrade soil. After placing the ballast and/or geotextile, a sinusoidal load was applied through a servo-controlled actuator. In this study, a uniform cyclic stress was applied as a minimum vertical stress (σ_{min} = 30 kPa), and the sinusoidal vertical cyclic stress (σ_{max} = 70 –140 kPa), thus simulates a maximum axle load of 35-40 tonnes. The frequency varied between 1.0 and 5.0 Hz, which represents the train speeds of 40-220 km/h in a typical railway track conditions (Powrie et al. 2007; Indraratna et al. 2020b).

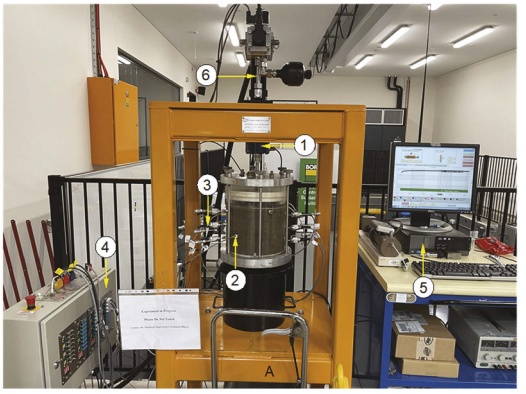

(1) Linear variable differential transformer (LVDT) and load cell,

(2) Miniature pore pressure transducers (MPs),

(3) Body pressure transducers (Ps),

(4) Lab controllers,

(5) Computer and Power supply and

(6) Hydraulic actuator

Figure 4. Dynamic filtration apparatus (DFA) at UTS-TRC.

2.2.4 *Experimental phases*

The laboratory tests were undertaken to simulate (a) undrained conditions where an impermeable boundary was created at the top of subgrade surface, and (b) free drainage conditions where a layer of ballast directly placed over the subgrade specimen. These two tests can be used to evaluate the failure criteria and subgrade fluidization. Dynamic filtration tests were carried out using geocomposite (T1), geotextile (T2) and PVD (P) and laid at the interface between the ballast and subgrade specimens to evaluate how well geosynthetics control the development of EPWP and preventing or delaying the initiation of subgrade fluidization. A series of laboratory experiments were undertaken to investigate the role of geotextiles and PVD under different axle loads and speeds. The loading frequency and amplitude applied varied from 1 to 5 Hz and 20-35 kPa (i.e., σ_{min}= 30 kPa, σ_{max} = 70-100 kPa), respectively. The effectiveness of a combined PVD-geocomposite system was also measured in terms of controlling the development of EPWP and mitigating/controlling the initiation of subgrade fluidization. A horizontal drainage path was created by the inclusion of PVD, and laboratory experiments were carried out to examine how effectively radial drainage could reduce the critical EPWPs that developed under cyclic load.

2.3 *Numerical modeling of subgrade fluidization*

In order to understand how the micro-structure of soil evolves under rising EPWP, a numerical investigation based on discrete element method (DEM) coupled with computational fluid dynamics (CFD) was carried out. In this approach, solid soil particles were modelled by DEM, while fluid flow was described by the CFD. Interactions between two phases, i.e., solid and fluid were governed through fluid-particle interaction models such as the pressure gradient, drag and viscous forces. Variables between the two computation platforms were exchanged regularly to ensure the effects from its counterpart to be captured properly. Details

of theoretical background and numerical algorithm of this method can be found in past studies of the Authors (Nguyen and Indraratna 2020; Nguyen and Indraratna 2022a). In the current paper, a sandy soil which is often used for capping layer under railways was simulated. Fluid went through the soil domain from the bottom to the top under increasing hydraulic gradient, while responses of soil and fluid at micro-scale were captured over time and space (Figure 5). It is important to note that a representative soil element was modelled in this case to enable particle-scale response of soil to be captured. Periodic boundary which simulated the continuous contacts between particles while migrating was used.

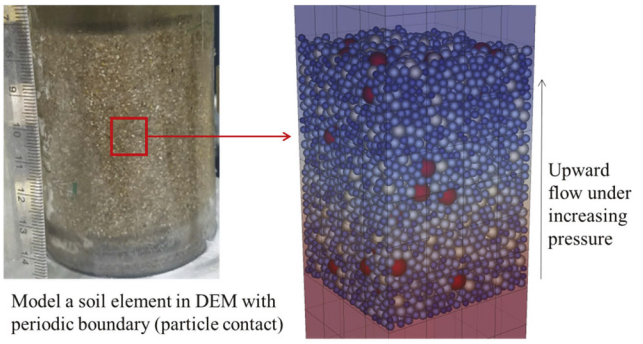

Figure 5. Numerical simulation of soil fluidization using CFD-DEM coupling.

3 RESULTS AND DISCUSSION

3.1 *Build-up of excess pore water pressure and migration of particles under cyclic loading*

When a specimen is subjected to increasing CSR, the specimen experiences larger deformations. However, there lies a critical cyclic stress ratio (CSR_c), wherein the mean excess pore pressure ratio (EPP) and cyclic axial strains shoot up rapidly. This is coupled with a sharp drop in the magnitude of the deviatoric stress q, indicating the onset of fluidization. Based on the test results, the CSR_c is dependent on the initial dry density of the soil specimen and the loading frequency. For example, as can be seen from Figure 6, the CSR_c for a specimen compacted at a dry density of 1790 kg/m^3 at a loading frequency of 1.0Hz lies between 0.4 and 0.5. Similar response was observed with soil samples collected from different mud pumping locations, despite different critical thresholds of load parameters and soil density (Indraratna et al. 2020a; Abeywickrama et al. 2021b).

The accumulation of excess pore water pressure governs the failure of the specimen under undrained cyclic loading. As seen from Figure 6, the increase in the CSR results in the increase in the build-up of excess pore water pressure. To quantify the effect of the EPWP, the incremental rate of EPWP was calculated. It is defined as the ratio between the EPWP and the log(N), where N is the number of cycles. It is observed that the rate of increment in EPWP at different CSRs (0.2, 0.3, and 0.4) is very similar (Figure 7a). The plots stabilize after the specimens reach 5% cyclic axial strain, and there is no considerable change after 2000 loading cycles. This implies that there is no further increase in the excess pore pressure. Figure 7b shows the variation of the incremental rate of EPWP with increasing CSR. When the specimen is subjected to a CSR = 0.5, there is a sudden increase in the excess pore pressure which results in the formation of slurry at the top of the specimen. For example, when the RC is 99%, the CSR_c lies between 0.4 and 0.5 for a frequency of 1.0 Hz. The CSR_c drops as the RC values reduces. It can be attributed to larger pore water pressure accumulation at lower RC as the specimen is in a relatively loose state.

A post-failure analysis was carried out for all fluidized specimens. Representative soil samples were carefully collected from the upper one-third and central region and were examined in the Malvern particle size analyzer. The results indicated an increase in the volume of fines (less than 75 microns) in the upper region of the specimen as opposed to the mid-region. This confirms that during the passage of trains, the fines migrate upwards and are transported by

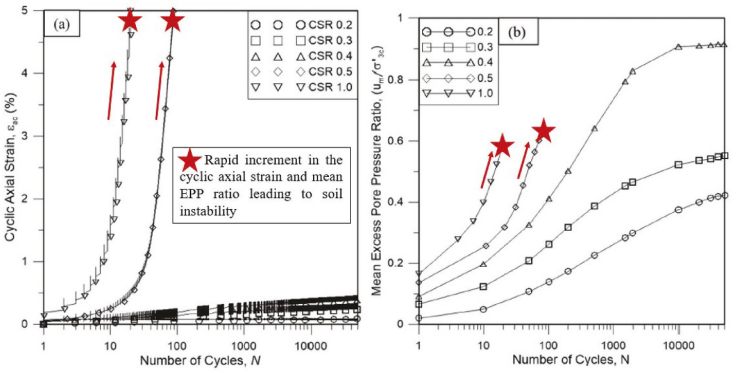

Figure 6. Generation of cyclic axial strains and mean excess pore water pressure (ρ_d = 1790 kg/m^3) (modified after Indraratna et al. 2020a).

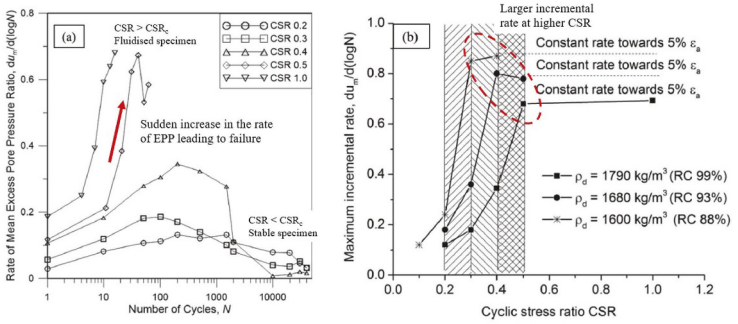

Figure 7. Variation in the incremental rate of EPWP with Number of cycles, N and CSR (modified after Indraratna et al. 2020a).

the displaced water which results in slurry formation or ponding of the slurry. Selig and Waters (1994) suggested that the cyclic nature of loading at the sleep-ballast interface generates a negative pressure which draws the suspended soil slurry from the subgrade level to the top of the ballast. Further, shallow subgrade with high water content (resulting from heavy rainfalls) during continuous railway loading may become susceptible to fluidization.

3.2 *Micromechanics of soil fluidization through numerical investigation*

The numerical results (Figure 8) show that when hydraulic gradient increases, soil particles are displaced under rising hydraulic forces acting on the particles, resulting in broken contact network and expanding porous system. For example, porosity of the simulated soil increases gradually under developing hydraulic gradient *i* before a sharp increase at the critical values of *i.* Meanwhile, the number of particle contacts drop immediately with rising *i* and become severe (i.e., the contact loss jumps from 20 to 35%) when *i* reaches the critical level (i.e., fluidization). While the change in porosity before the onset of fluidization is usually hard to measure in conventional laboratory due to its very sensitive magnitude, the response from particle contact network captured in the current CFD-DEM coupling model is apparent even at a small level of excess pore water pressure gradient or internal *i*. When the effective contacts of particles (i.e., the contacts bear effective stresses) are significantly vanished, soil behaves likes fluid with floating particles, thus fluidization. This microscale analysis indicated that preventing the accumulated EPWP and/or reinforcing contact network of soil are certainly effective approaches to mitigate particle migration and soil softening under rail tracks.

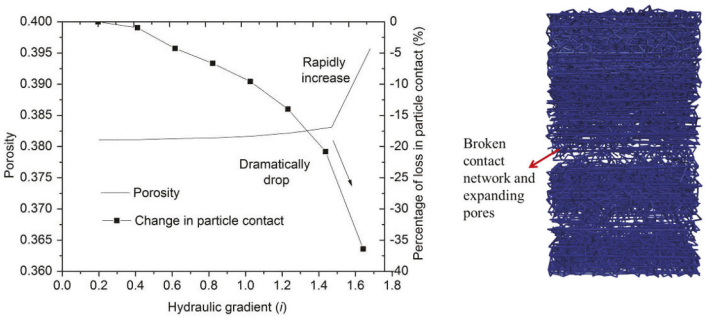

Figure 8. Degradation in micro-structure (porosity and particle contact) of soil under rising internal pore water pressure.

3.3 *Stabilization of subgrade soil using membrane and the composite membrane PVDs*

3.3.1 *Effectiveness of geosynthetics under cyclic loading*

The EPWPs that developed inside the specimen were measured because they were the main cause of instability in soft subgrade under continuous cyclic loading. Figure 9(a) shows the rapid development of EPWPs up to 500 cycles, where all the miniature pressure readings remain above 30 kPa when using geocomposite T1. The transducer MP2 (at 40 mm) measured the maximum EPWP of 37 kPa at 500 cycles. However, geocomposite with a filter membrane (AOS <10 μm) could dissipate the EPWPs below 10 kPa at the end of 75,000 cycles. When only using a geocomposite, the rate of excess pore water dissipation in Test T1 was higher near the ballast/subgrade interface (MP1) than the middle/shallow part of the subgrade (MP2 and MP3). In Test T2, until the test reached 65,000 cycles, the values from MP2 measured 40 mm below the interface were more than 20 kPa for T2 and with a very low rate of dissipation compared to geocomposite T1. As Figure 9(a) shows, T1 dissipated EPWPs by more than 76% and 52%, at 20 and 40 mm below the interface, unlike geotextile T2 at 75,000 cycles. This indicates that geocomposite (T1) dissipated the EPWP better than in comparison to conventional geotextile T2.

Undrained cyclic tests (impermeable boundary created by a geomembrane) indicated that the EPWPs that develops inside the soil specimen without a significant reduction over time might cause subgrade instability (Singh et al. 2020; Arivalagan et al. 2021). As shown in Figure 9(a), the magnitudes of EPWP that developed in Test T1 are more than 30 kPa at 500 cycles at all three depths; however, the presence of PVD (Test P+T1) certainly dissipates the EPWPs, especially in the deeper layers of soil. Therefore, the values of EPWPs from Test P+T1 are less than 15 kPa within 500 cycles and less than 4 kPa after 75,000 cycles. In other words, although a sole geotextile (Test T2) shows a maximum EPWP of more than 15 kPa at 75,000 cycles, there is approximately 80% reduction in EPWPs 40 mm under the interface due to the inclusion of the PVD-geocomposite system as shown in Figure 9(a) (i.e., the EPWPs at MP2 and MP3 remain below

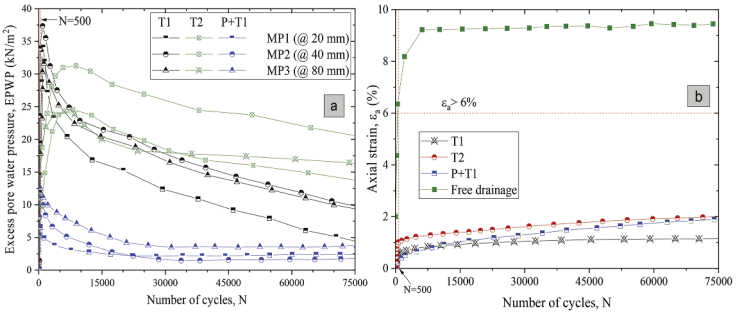

Figure 9. Generation of (a) EPWPs and (b) axial strains with geocomposite (T1), geotextile (T2), and a combined PVD-geocompoite system (after Arivalagan et al. 2022).

5 kPa). This proves that a combined PVD and geocomposite (P+T1) system can reduce the potential for subgrade fluidization during cyclic loading due to the continuous dissipation in EPWPs.

As Figure 9(b) shows, the maximum axial strain (ε_a > 6%) in free drainage tests (35 mm thick ballast was directly placed over the subgrade surface) only occurred after 500 cycles. However, the development of axial strain was controlled due to the inclusion of geotextiles at the interface. Geocomposite (T1) could provide more confinement at the ballast/subgrade interface and prevent the penetration of coarser ballast particles into the subgrade soil in Test T1. However, there was a continual increase in axial deformation due to the migration of fine particles through the pore openings of geotextile (T2) and the residual axial strain after 75,000 cycles remained above 2% for T2. This may lead to differential settlements in railway tracks under repeated cyclic loading conditions.

3.3.2 *Performance of geocomposites under varying cyclic stress*

A set of cyclic deviatoric stresses (i.e., σ_{max} of 70 and 100 kPa) were used to demonstrate how an increased axle load affects the cyclic behaviour of subgrade soil, and to assess the effectiveness of geocomposite T1. There was an expeditious development in EPWPs when the cyclic deviator stress increased up to 100 kPa when a sole geocomposite placed on the subgrade. As shown in Figure 10(a), geocomposite T1 could not reduce the cyclic EPWPs effectively at the middle to the lower region (i.e., the critical layers) when the cyclic stress increased to 100 kPa. The readings from miniature pressure transducers MP2, MP3, and MP4 remained above 35 kPa until the test ended and these results imply that an increased axle load in railway tracks (35-40 tonnes) generates a rapid increase in EPWPs, and the inclusion of geocomposite cannot dissipate them quickly under adverse hydraulic conditions. The increasing trend in axial strain was reported in previous studies when soft subgrade soil is subjected to a higher cyclic stress (Indraratna et al. 2020a). A similar increasing trend was observed at 100 kPa, where ε_a reached 5% before 75,000 cycles, as shown in Figure 10(b). The axial strain for 70 kPa (maximum vertical stress) was less than 1.5% until the test ended, but it rocketed up to 5.3% at 80,000 cycles at 100 kPa maximum vertical stress. Although geocomposite can mitigate the migration of fine particle at 70 kPa, a lot of fine particles accumulated during higher cyclic stress (under 35-40 tonnes axle load), which may induce subgrade instability due to excessive deformation in railway tracks.

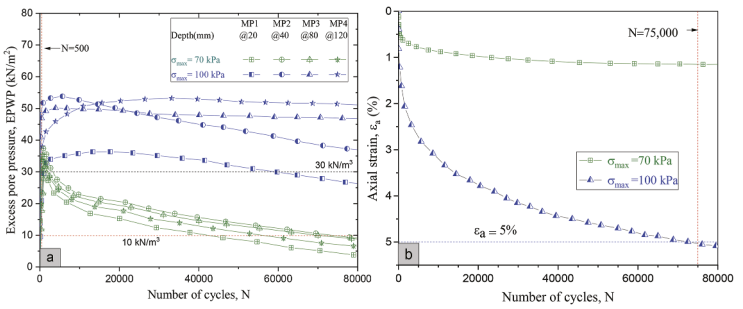

Figure 10. (a) Generation of EPWPs and (b) axial strains due to the inclusion of geocomposite (T1) under different cyclic stress (i.e. σ_{min} = 30 kPa, σ_{max} = 70 - 100 kPa) (modified after Arivalagan et al. 2021).

3.3.3 *The role of PVD-geocomposite system in a typical railway track*

The significant variation in drainage conditions at the interface and inside the soil were studied based on the generation of an excess pore pressure gradient (EPPG) at different depths. The EPWP measured at different soil layers by pressure transducers were used to calculate the EPPG. This can be defined as the ratio between changes in the excess pore water pressure head (unit = m head) and the corresponding distance between two specified locations (unit = m). The generation of critical EPPGs at various locations (inside the subgrade) can also induce instability by dislocating the fines from the original soil matrix. As Figure 11(a) shows, EPPG that developed in undrained tests rocketed above 40 after 500 cycles, and there was no significant reduction until

15,000 cycles. This non-uniform development of EPPGs in the middle and deeper subgrade soil, i.e., Layers (2-1) and (3-2), created a significant upward hydro-dynamic force that dislocated the finer particles towards the top layers. However, a PVD-geocomposite system (P+T1) reduced the EPPG at the top three layers of the soil within 2500 cycles. The EPPGs that developed in Layers (2-1) and (3-2) decreased by 67% and 90% due to the inclusion of PVD and geocomposite (T1), as shown in Figure 11(a). In addition, EPPG that developed at the middle and lower regions (Layer (3-2) and Layer (4-3)) was less than five until the end of cyclic tests.

The increase in the fine percentage and the formation of slurry at the interface (abrupt change in the water of soil) were used to assess the potential for subgrade fluidization in several studies (Indraratna et al. 2020b). Therefore, PSD and moisture content tests were conducted after each cyclic test. Malvern particle size analyzer was used to measure the particle size distributions at the top, middle, and bottom regions at the end of loading. Figure 11(b) shows that fine particles of less the 75μm had accumulated at the top surface in undrained tests where a lot more fines were lost in the middle layers (between 1 and 60μm) compared to the initial PSD. As shown in Figure 11(b), the inclusion of P+T1 prevented the migration of particles from the middle and lower regions. There were no significant variations in PSD, especially at the top and middle layers. This shows that PVD and geocomposite with an effective filter (P+T1) can prevent particle dislocation under critical hydro-dynamic conditions. Similarly, there was a large accumulation of fines (less than 1μm) in the top and middle layers in Test T2. Moreover, the water content for undrained and free drainage tests were close to the liquid limit at the top surface of the subgrade and the amount of high water near the interface causes softening and can induce fluidization as finer particles accumulate below 500 cycles. However, a PVD-geocomposite system helped to reduce the water content where they had a maximum water content of 30% near the interface, which prevented the soil softening under cyclic loading.

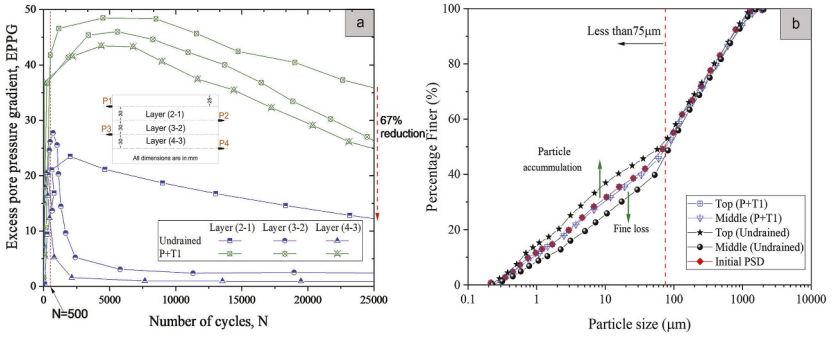

Figure 11. Undrained cyclic test and a combined PVD-geocomposite system (a) EPPGs and (b) variations in PSD (modified after Arivalagan et al. 2022).

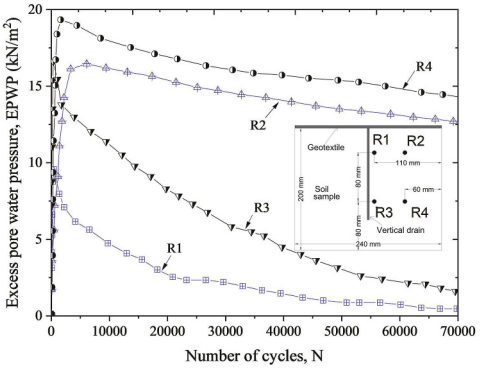

Figure 12. Dissipation of EPWPs due to radial drainage paths (P+T1).

Transducers (MPs) were installed at different locations from the centre (in radial direction 0 and 60 mm from the centre line) to measure how much the prefabricated vertical drains could alleviate the EPWPs (Figure 12). The EPWP measured at R1 (i.e., the shortest radial drainage path) is lower than at R2. Although the EPWPs developed at location R4 may take much longer to dissipate than R3, the PVDs successfully dissipate them before reaching their critical values. Furthermore, the EPWPs that developed at R1 and R3 approached zero after 70,000 cycles. The EPWPs measured at R2 and R4 decreased continuously as the number of cycles increased and were less than 14 kPa at the end of cyclic loading. Furthermore, PVDs can continually alleviate EPWPs during train loading and even during the rest period after each train passes.

3.3.4 *Effectiveness of PVD-geocomposite system under different axle loads and frequencies*
Figure 13(a) shows that the rapid generation of EPWP at 40 mm below the subgrade interface approached 50 kPa prior to reaching 5000 cycles when the maximum vertical stress increased to 100 kPa (approximately 35 tonnes axle loading). However, the EPWPs in the top and middle layers continued to dissipate due to the application of a PVD-geocomposite system. For instance, the EPWPs that developed at MP1 and MP3 were less than 25 kPa under varying cyclic stresses at the end of each cyclic test. In essence, the rapid generation of axial strain was controlled using geosynthetics because the axial strain was only 3% and 2.2% after 100,000 cycles at 30 and 35 tonnes axle loads, respectively. Figure 13(b) shows the effects of two different frequencies with the combination of PVD and geocomposite system. The results indicated that EPWPs that developed at all three locations (MP1, MP2 and MP3) decreased at a lower frequency. An increase in frequency (f=5 Hz) causes a significant increase in EPWPs at MP1 compared to the test under 3 Hz frequency. In addition, the rate of dissipation of EPWP is slightly higher in the test carried out at a lower frequency. The EPWPs that developed at MP1 are 4 kPa and 5 kPa for F=3 and 5 Hz at the end of the cyclic tests (Figure 13(b)). These results confirmed that a PVD-geocomposite system can still prevent critical EPWP generation even under higher frequencies.

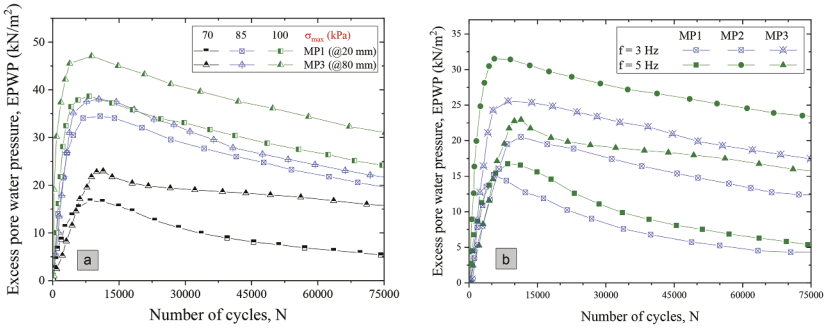

Figure 13. Performance of a combined PVD-geocomposite system under different (a) cyclic stresses (i.e. σ_{min} = 30 kPa, σ_{max} = 70 - 100 kPa) and (b) frequencies (3-5 Hz) (modified after Arivalagan et al. 2022).

4 CONCLUSIONS AND INDUSTRY IMPACT

Comprehensive experimental and numerical studies were carried out to investigate the mechanism and causative factors of subgrade fluidization under heavy haul trains. Geosynthetics and PVD-geocomposite inclusions to mitigate subgrade fluidization were proposed and examined through a large-scale model test. Salient findings of this study can be summarized as follows:

(1) The passage of heavy freight trains can cause a non-uniform accumulation of EPWP over the depth of subgrade soil, resulting in increasing excess pore pressure gradient (EPPG or an internal hydraulic gradient). When this gradient reached a critical level, the internal flows brought moisture and fines upward accompanied with stiffness degradation, thus

mud pumping. The heaver the train, the larger the cyclic stress ratio, the larger the accumulated EPWP and EPPG.

(2) The numerical investigation at micro-scale showed that increasing internal hydraulic gradient meant larger hydraulic forces acting on soil particles that pushed particles away while expanding the pore network (i.e., increasing porosity). As this continued to develop under repeated loading, the soil matrix significantly lost effective contacts between particles that resulted in reduced stiffness and fluidized soil.

(3) Increasing the relative compaction (or density) of soil can enhance the resistance to fluidization, however, when the axle load exceeded very high degree (CSR > 0.5), additional soil stabilization such as inclusion of geosynthetics should be considered.

(4) PVDs combined with a drainage membrane (geocomposite at the interface) facilitated the dissipation of EPWP and EPPG that significantly enhanced track stability by preventing soil softening and fluidization. The test results showed that a combined PVD-geocomposite system can effectively dissipate the pore water pressure even when the axle load and frequency reached high degrees (e.g., equivalent 35-40 tons and 120 km/h train speed over 75,000 loading cycles).

ACKNOWLEDGEMENT

Financial and technical support provided by the Australian Research Council (ARC) funded ITTC-Rail (i.e., LP160101254, LP200200915, DP220102862, IC170100006), and industry partners including TetraTech Coffey, SMEC, ACRI, Sydney Trains and Global Synthetics is gratefully acknowledged. The authors would also like to acknowledge the assistance provided by EngAnalysis for the installation of instrumentation at Chullora Technology Precinct. Some contents of this paper have been published earlier in scholarly journals and reproduced herein with kind permission from Canadian Geotechnical Journal, Geotextiles and Geomembranes Journal, Transportation Geotechnics Journal, among others.

REFERENCES

Abeywickrama, A., Indraratna, B., Nguyen, T.T. and Rujikiatkamjorn, C. 2021b. Laboratory investigation on the use of vertical drains to mitigate mud pumping under rail tracks. *Australian Geomechanics Journal*, **56**(3): 117–126.

Arivalagan, J., Indraratna, B., Rujikiatkamjorn, C. and Warwick, A. 2022. Effectiveness of a Geocomposite-PVD system in preventing subgrade instability and fluidisation under cyclic loading. *Geotextiles and Geomembranes*, **50**(4): 607–617.

Arivalagan, J., Rujikiatkamjorn, C., Indraratna, B. and Warwick, A. 2021. The role of geosynthetics in reducing the fluidisation potential of soft subgrade under cyclic loading. *Geotextiles and Geomembranes*, **49**(5): 1324–1338. https://doi.org/10.1016/j.geotexmem.2021.05.004.

ASTM D638-03. 2003. Standard Test Method for Tensile Properties of Plastics. ASTM International, 100 Barr Harbor Drive, PO Box C700, West Conshohocken, PA 19428-2959, United States.

ASTM D3774-96. 1996. Standard Test Method for Width of Textile Fabric. ASTM, 100 Barr Harbor Drive, West Conshohocken, PA 19428-2959, United States.

ASTM D3999-91. 2003. Standard Test Methods for the Determination of the Modulus and Damping Properties of Soils using the Cyclic Triaxial Apparatus. Annual Book of ASTM standards.

ASTM D4716-00. 2000. Standard Test Method for Determining the (In-plane) Flow Rate per Unit Width and Hydraulic Transmissivity of a Geosynthetic Using a Constant Head. ASTM International, United States.

ASTM D4751-99. 1999. Standard Test Method for Determining Apparent Opening Size of a Geotextile. ASTM, 100 Barr Harbor Drive, West Conshohocken, PA 19428-2959, United States.

ASTM D5199-01. 2001. Standard Test Method for Measuring the Nominal Thickness of Geosynthetics. ASTM, 100 Barr Harbor Drive, West Conshohocken, PA 19428-2959, United States, Pa.

ASTM F316-03. 2011. Standard Test Methods for Pore Size Characteristics of Membrane Filters by Bubble Point and Mean Flow Pore Test. ASTM International, West Conshohocken, PA, 2003.

Chawla, S. and Shahu, J.T. 2016. Reinforcement and mud-pumping benefits of geosynthetics in railway tracks: Model tests. *Geotextiles and Geomembranes*, **44**(3): 366–380. https://doi.org/10.1016/j.geotexmem.2016.01.005.

Duong, T.V., Tang, A.M., Cui, Y.-J., Trinh, V.N., Dupla, J.-C., Calon, N., Canou, J. and Robinet, A. 2013. Effects of fines and water contents on the mechanical behavior of interlayer soil in ancient railway sub-structure. *Soils and Foundations*, **53**(6): 868–878. https://doi.org/10.1016/j.sandf.2013.10.006.

EN ISO 9863-1. 2005. Geosynthetics–Determination of thickness at specified pressures. Part 1: Single Layers. CEN, Brusel.

EN ISO 10319. 2008. Geosynthetics–Wide-width tensile test. International Organization for Standardization, Geneva, Switzerland.

EN ISO 11058. 2019. Geotextiles and geotextile-related products — Determination of water permeability characteristics normal to the plane, without load. ISBN 978 0 580 93628 9, Pa.

EN ISO 12236. 2006. Geosynthetics—Static Puncture Test (CBR Test). European Committee for Standardization, Brussels, Belgium.

EN ISO 13433. 2006. Geosynthetics-Dynamic perforation test (cone drop test). ISO/TC 221 Geosynthetics, ISO 13433:2006.

Giroud, J. 1996. Granular filters and geotextile filters. *Geofilters 96, Proc. of 2nd Int. Conf." Geo-filters"*: 565–680.

Hudson, A., Watson, G., Le Pen, L. and Powrie, W. 2016. Remediation of Mud Pumping on a Ballasted Railway Track. *Procedia Engineering*, **143**: 1043–1050. https://doi.org/10.1016/j.proeng.2016.06.103.

Hyodo, M., Yamamoto, Y. and Sugiyama, M. 1994. Undrained Cyclic Shear Behaviour of Normally Consolidated Clay Subjected to Initial Static Shear Stress. *Soils and Foundations*, **34**(4): 1–11. https://doi.org/10.3208/sandf1972.34.4_1.

Indraratna, B., Attya, A. and Rujikiatkamjorn, C. 2009. Experimental investigation on effectiveness of a vertical drain under cyclic loads. *Journal of geotechnical and geoenvironmental engineering*, **135**(6): 835–839.

Indraratna, B., Korkitsuntornsan, W. and Nguyen, T.T. 2020a. Influence of Kaolin content on the cyclic loading response of railway subgrade. *Transportation Geotechnics*, **22**: 100319. https://doi.org/10.1016/j.trgeo.2020.100319.

Indraratna, B., Nimbalkar, S. and Rujikiatkamjorn, C. 2014. From theory to practice in track geomechanics – Australian perspective for synthetic inclusions. *Transportation Geotechnics*, **1**(4): 171–187. https://doi.org/10.1016/j.trgeo.2014.07.004.

Indraratna, B., Singh, M., Nguyen, T.T., Leroueil, S., Abeywickrama, A., Kelly, R. and Neville, T. 2020b. Laboratory study on subgrade fluidization under undrained cyclic triaxial loading. *Canadian Geotechnical Journal*, **57**(11): 1767–1779.

Ito, T. 1984. Actual situation of mud pumping and its countermeasures. *Quarterly Reports of the Railway Technical Research Institute*, **25**(4): 117–123.

Kermani, B., Stoffels, S. and Xiao, M. 2020. Evaluation of effectiveness of geotextile in reducing subgrade migration in rigid pavement. *Geosynthetics International*, **27**(1): 97–109.

Lenart, S., Bizjak, K.F., Noren-Cosgriff, K., Kaynia, A.M., Kramar, M., Vajdić, M., Chen, K. and Clarke, J. 2018. Guidelines on the use of novel construction and maintenance techniques within the operational railway environment. *DESTination RAIL – Decision Support Tool for Rail Infrastructure Managers*.

Nguyen, T.T. and Indraratna, B. 2020. A coupled CFD-DEM approach to examine the hydraulic critical state of soil under increasing hydraulic gradient. *ASCE International Journal of Geomechanics*, **20**(9):04020138-1:15. https://doi.org/10.1061/(ASCE)GM.1943-5622.0001782.

Nguyen, T.T. and Indraratna, B. 2022a. Fluidization of soil under increasing seepage flow: an energy perspective through CFD-DEM coupling. *Granular Matter*, **24**(3): 80. doi: 10.1007/s10035-022-01242-6.

Nguyen, T.T. and Indraratna, B. 2022b. Rail track degradation under mud pumping evaluated through site and laboratory investigations. *International Journal of Rail Transportation*, **10**(1): 44–71. doi: 10.1080/23248378.2021.1878947.

Nguyen, T.T., Indraratna, B., Kelly, R., Phan, N.M. and Haryono, F. 2019. Mud pumping under railtracks: Mechanisms, Assessments and Solutions. *Australian Geomechanics Journal*, **54**(4): 59–80.

Nguyen, T.T., Indraratna, B. and Leroueil, S. 2022. Localized behaviour of fluidized subgrade soil subjected to cyclic loading. *Canadian Geotechnical Journal*, **59**. https://doi.org/10.1139/cgj-2021-0550.

Ni, J. 2012. Application of geosynthetic vertical drains under cyclic loads in stabilizing tracks. *PhD Thesis*, *University of Wollongong*, *Australia, p.* 210.

Polito, C.P. and II, J.R.M. 2001. Effects of Nonplastic Fines on the Liquefaction Resistance of Sands. *Journal of Geotechnical and Geoenvironmental Engineering*, **127**(5): 408–415. doi: 10.1061/(ASCE)1090-0241(2001)127:5(408).

Powrie, W., Yang, L. and Clayton, C.R. 2007. Stress changes in the ground below ballasted railway track during train passage. *Proceedings of the Institution of Mechanical Engineers, Part F: Journal of Rail and Rapid Transit*, **221**(2): 247–262.

Raymond, G.P. 1986. Geotextile Application for a branch line upgrading. *Geotextiles and Geomembranes*, **3**(2): 91–104. https://doi.org/10.1016/0266-1144(86)90002-6.

Sakai, A., Samang, L. and Miura, N. 2003. Partially-drained cyclic behaviour and its application to the settlement of a low embankment road on sitly-clay. *Soils and Foundations*, **43**(1): 33–46. doi: 10.3208/sandf.43.33.

Selig, E.T. and Waters, J.M. 1994. Track geotechnology and sustructure management. Thomas Telford, London.

Sharpe, P., Roskams, T. and Valero, S.N. 2014. The development of a geocomposite to prevent mud pumping. In *Proceedings of the Conference on Railway Excellence: Railway Transport for Vital Economy (RTSA)*, Adelaide, Australia. pp. 346–353.

Silva, I.N., Indraratna, B., Nguyen, T.T. and Rujikiatkamjorn, C. 2022. Shear behaviour of subgrade soil with reference to varying initial shear stress and plasticity index. *Acta Geotechnica*. https://doi.org/10.1007/s11440-022-01477-w.

Singh, M., Indraratna, B., Rujikiatkamjorn, C. and Kelly, R. 2020. Cyclic response of railway subgrade prone to mud pumping. *Australian Geomechanics Journal*, **55**(1): 43–54.

Transport for NSW. 2016. Track Reconditioning Guidelines, T HR CI 12120 GU. Transport Asset Standards Authority, NSW.

Vucetic, M. and Dobry, R. 1991. Effect of Soil Plasticity on Cyclic Response. *Journal of Geotechnical Engineering*, **117**(1): 89–107. doi: 10.1061/(ASCE)0733-9410(1991)117:1(89).